SPANDIDOS PUBLICATIONS

EXPERIMENTAL AND THERAPEUTIC MEDICINE 15: 2703-2710, 2018

Roles of autophagy in androgen-induced benign prostatic hyperplasia in castrated rats

RONG-FU LIU, GUO FU, JIAN LI, YU-FENG YANG, XUE-GANG WANG, PEI-DE BAI and YUE-DONG CHEN

Department of Urology, The First Affiliated Hospital of Xiamen University, Xiamen, Fujian 361003, P.R. China

Received May 9, 2016; Accepted March 31, 2017

DOI: 10.3892/etm.2018.5772

Abstract. The present study investigated the role of androgen in the process of androgen-induced prostate hyperplasia in castrated rats and assessed the role of the phosphoinositide 3-kinase/protein kinase B/mechanistic target of rapamycin (PI3K/Akt/mTOR) pathway in this process. Furthermore, the extent to which autophagy may affect the level of androgen-induced benign prostatic hyperplasia was also explored. A total of 40 Sprague Dawley rats were randomly divided into four groups: Testosterone group, rapamycin group, 3-methyladenine (3-MA) group, and control group. The extent of hyperplasia in prostate tissue the apoptosis and autophagy were assayed. The prostate wet weight, volume and index in the testosterone group were significantly higher compared with the control group ($P<0.05$) and these factors were significantly lower in the rapamycin group compared with the testosterone group ($P<0.05$). HE staining demonstrated that prostate hyperplasia was obvious in the testosterone group. Western blotting revealed that caspase-3 levels were higher in the 3-MA group compared with the control group and Bcl-2 was higher in the testosterone group compared with the control group ($P<0.05$). Furthermore, in the rapamycin group, Bcl-2 protein expression levels were significantly lower than those in the testosterone group ($P<0.05$). The prostate tissue was analyzed using electron microscopy and autophagy bodies were identified in the rapamycin group. In the process of androgen-induced prostatic hyperplasia in castrated rats, the role of androgen may be related to the PI3K/Akt/mTOR signaling pathway. Rapamycin was able to inhibit the effect of testosterone and promoted prostate tissue hyperplasia by inhibiting the PI3K/Akt pathway. In addition to inhibiting apoptosis in prostate cells, androgen was able to induce rat prostate hyperplasia and may also be related to the promotion of the proliferation of prostate cells.

Correspondence to: Professor Rong-Fu Liu, Department of Urology, The First Affiliated Hospital of Xiamen University, 55 Zhen Hai Road, Xiamen, Fujian 361003, P.R. China
E-mail: lliurf@126.com

Key words: androgen signaling pathway, benign prostatic hyperplasia, apoptosis, castrated rats

Introduction

Benign prostatic hyperplasia (BPH) is a common disease in men >50 years of age as the incidence of the disease increases with age (1). BPH can seriously affect the quality of life of patients with common clinical manifestations, including dysuria, urinary frequency, urgency, urinary incontinence, and other lower urinary tract symptoms (2). Severe cases may cause urinary tract infections, urinary tract obstruction, bladder stones, renal failure and other adverse effects (2). Epidemiological studies have suggested that risk factors for BPH include heredity, nutrition, and immunity (3,4). Recent studies suggest that BPH is also closely associated with metabolic syndromes, such as obesity, hyperglycemia, dyslipidemia and hypertension; it is also associated with secondary urinary tract syndrome secondary to BPH (5).

At present, treatment of BPH consists primarily of drug therapy and surgical treatment. Given the critical role of androgens, derived largely from the testis with a small amount (~1%) from the adrenal gland (6), in regulating prostate tissue growth, 5-alpha reductase inhibitors (5-ARI) constitute the only drug that reduces the size of the prostate gland by lowering the level of dihydrotestosterone. However, 5-ARI therapy is slow, requiring at least three months before it works, and only reduces prostate volume by 20% (7,8).

The development of new therapeutic approaches requires a detailed examination of the underlying pathogenic processes. Although the pathogenesis of BPH has not been fully elucidated at present, pathological changes associated with BPH include prominent glandular hyperplasia with stromal hyperplasia (9). The most commonly used animal model is a rat model of androgen-induced prostate hyperplasia. A study by Scolnik *et al* (10) demonstrated that Sprague Dawley (SD) or Wistar rats injected with exogenous androgen after castration resulted in the proliferation of rat prostate tissue, an effect that was stable with good reproducibility.

The present study was undertaken to investigate the role of androgens in androgen-induced BPH in castrated rats and to evaluate the role of the phosphoinositide 3-kinase/protein kinase B/mechanistic target of rapamycin (PI3K/Akt/mTOR) pathway in this process. The role of autophagy in androgen-induced BPH was also determined. In the present study, androgens induced glandular hyperplasia, which may be mediated by inhibiting prostate cell apoptosis and promoting the proliferation of prostate cells. A role for the PI3K/Akt/mTOR signaling

pathway in androgen-induced BPH was also demonstrated. These results may form the basis of further clinical studies analyzing these pathways as potential therapeutic targets for BPH treatment.

Materials and methods

Animals. A total of 40 healthy male SD rats (age, 8 weeks; weight, 250±10 g) were provided by the Experimental Animal Center of Xiamen University (Xiamen, China). Rats were housed in an air-conditioned atmosphere at 22˚C and 50% relative humidity in a specific pathogen-free controlled room with a 12 h light/dark cycle and provided with unrestricted amount of rodent chow and water. All experimental procedures were conducted in conformity with institutional guidelines for the care and use of laboratory animals, and protocols were approved by the Institutional Animal Care and Use guidelines in The First Affiliated Hospital of Xiamen University (Xiamen, China). The study was approved by the Ethics Committee of The First Affiliated Hospital of Xiamen University (Xiamen, China).

Male SD rats were randomly divided into four groups (n=10 per group): The testosterone group (received bilateral testicular resection and subcutaneous injection of testosterone), rapamycin group (received bilateral testicular resection, subcutaneous injection of testosterone and intraperitoneal injection of rapamycin), 3-MA group (received bilateral testicular resection, subcutaneous injection of testosterone and intraperitoneal injection of 3-MA) and control group [received bilateral testicular resection, subcutaneous injection with solvent (90% olive oil and 10% ethanol) and intraperitoneal injection of normal saline]. To establish a BPH model, rats in all of the groups underwent bilateral testicular resection following administration of anaesthetic, as previously described (6,11). At day 25 following surgery, rats in the testosterone, rapamycin and 3-MA groups were injected with 0.5 mg/day testosterone propionate (Sigma-Aldrich; Merck KGaA Darmstadt, Germany) in the hind leg. Following establishment of the BPH model, the testosterone group was injected intraperitoneally with normal saline (1 mg/kg/day), the rapamycin group was injected intraperitoneally with rapamycin (1 mg/kg/day; Sigma-Aldrich Merck KGaA) and the 3-MA group was injected intraperitoneally with 3-MA (1 mg/kg/day; Sigma-Aldrich; Merck KGaA). In the control group, the scrotum skin was sutured after the testes of rats were detached, and the rats received an intraperitoneal injection of 1 mg/day normal saline as well as a subcutaneous injection in the hind leg with 1 ml solvent (90% olive oil and 10% ethanol) immediately following the surgery. Treatments were administered for 28 days.

Investigation of prostate index. Rats in each group were weighed 28 days after feeding. Rats were sacrificed by intraperitoneal injection using 100 mg/kg Nembutal (Beijing Genia Biotechnology, Co., Ltd., Beijing, China) and the prostate tissues were removed. The weight of the prostate tissue after cleaning the blood with filter paper was measured and the volume of the prostate was measured using the displacement method after submerging the tissue in a water-filled graduated cylinder. The left and right ventral lobes of the prostate were stored in liquid nitrogen or 10% formaldehyde solution, respectively.

Hematoxylin and eosin (HE) staining. Prostate tissues from rats in each group were fixed in 10% formalin at 4˚C overnight, and were then washed with PBS. The blocks were then dehydrated in graded alcohols, cleared in xylene and embedded in paraffin wax. The paraffin blocks were cut it into sections of 6 μm thickness and stained with HE. Briefly, the sections were dewaxed with xylene and dehydrated using graded ethanol, followed by washing with distilled water. The sections were sequentially transferred and washed after each step as follows: hematoxylin solution for 1 min, 1% hydrochloric acid solution for 10 sec, 1% ammonia complex blue for 30 sec, and 0.5% eosin solution for 2 min in thermostat with temperature 40˚C. After ethanol dehydration, the extent of hyperplasia, as a percentage of hyperplastic tissue in the whole section was observed using an optical microscope (Nikon Eclipse 50i, Nikon Corporation, Tokyo, Japan).

Western blotting to determine protein expression levels of B-cell lymphoma 2 (Bcl-2) and microtubule-associated protein 1 light chain 3 (LC3)-II in rat prostate tissues. Proteins were isolated from rat prostate tissues following snap freezing by immersion in liquid nitrogen. For 5 mg of tissue, 300 μl of ice-cold RIPA lysis buffer (cat no. 89900; Thermo Fisher Scientific, Inc.) was rapidly added. Following homogenization with a blade that was rinsed twice (200 μl each) with lysis buffer, the homogenate was maintained under constant agitation for 2 h at 4˚C. Protein concentrations were determined using a Pierce BCA Protein assay kit, according to the manufacturer's protocol. After the addition of protein loading buffer and boiling for 10 min, 50 μg of lysate was loaded and separated using 10-15% SDS-PAGE and transferred to nitrocellulose membranes. All further incubations were performed at room temperature on a platform shaker. Membranes were blocked with TBS supplemented with 0.1% Tween-20 (v/v) and 5% (w/v) non-fat dry milk for 30 min at room temperature prior to incubation with the following primary antibodies for 12 h: Anti-LC3 (cat no. 3868; Cell Signaling Technology, Danvers, MA, USA; 1:1,000); anti-Beclin-1 (cat no. ab62557; Abcam; Cambridge, MA, USA, 1:1,000) and anti-caspase-3 (cat no. ab32351; Abcam; 1:1,000). The blots were washed three times with wash buffer (5-10 min each). Subsequently, the membranes were incubated with anti-rabbit immunoglobulin horseradish peroxidase-conjugated secondary antibodies (cat no. sc-2030 and cat no. sc-2005; Multisciences Biotech Co., Ltd., Hangzhou, China, 1:10,000) for 2 h. GAPDH (cat no. ab9485; Abcam, 1:1,000) was used as an internal reference. After washing the blot four times with wash buffer (5-10 min each), immunoreactive proteins were visualized by enhanced chemiluminescence (Perkin Elmer, Shelton, CT, USA).

Detection of Bcl-2 and Beclin1 mRNA expression levels in rat prostate tissues by reverse transcription-quantitative polymerase chain reaction (RT-qPCR). RNAs were isolated and purified from rat prostate tissues using a RNeasy Mini kit (cat no. 74104; Qiagen AB, Sollentuna, Sweden). For Complementary DNA synthesis, reverse transcription was performed using the Prime Script RT Reagent kit (Takara Bio

Inc., Otsu, Japan) according to the manufacturer's protocols. For reverse transcription, the reaction mixtures was incubated under the following conditions: 1 cycle of 37˚C for 15 min; 1 cycle of 85˚C for 5 sec and 1 cycle of 4˚C for 10 min. Primers were designed by the GenScript PCR Primer Design Tool (http://www.genscript.com/) and were synthesized by Shanghai GenePharma Co., Ltd. (Shanghai, China). The primer sequences were as follows: β-actin, forward, 5'-GAA GATCAAGATCATTGCTCCT-'3 and reverse, 5'-TACTCC TGCTTGCTGATCCA-3'; Bcl-2, forward, 5'-TAAGCTGTC ACAGAGGGGCT-'3 and reverse, 5'-GCGACGAGAGAA GTCATCCC-3'; and Beclin1, forward, 5'-GGCTGAGAG ACTGGATCAGG-3' and reverse, 5'-CTGCGTCTGGGC ATAACG-3'. qPCR was performed using SYBR Premix EX TaqII (Takara, Shiga, Japan) following the manufacturer's instructions. Each 30-μl reaction contained 0.4 μM primer pairs, 100 ng cDNA, 15 μl SYBR Green, and 0.6 μl ROX as a fluorescence internal control. The amplification program comprised of two stages. The first Tag activation stage began with an initial 95˚C for 10 min followed by 40 cycles of denaturation at 95˚C for 5 sec and annealing at 60˚C for 40 sec. Subsequently, a melting curve analysis was performed by collecting fluorescence data. The relative T/S values were calculated according to the $2^{-\Delta\Delta Cq}$ method (12).

Detection of apoptosis in rat prostate tissue by terminal deoxynucleotidyl transferase dUTP nick-end labeling (TUNEL) assay. TUNEL was performed according to the instructions of the TUNEL cell apoptosis detection kit (cat no. 11684795910; Roche Molecular Diagnostics, Branchburg, NJ, USA). Exposed 3'-OH of genomic DNA were broken and terminal deoxynucleotidyl transferase enzyme catalysis and DUTP (fluorescein-dUTP) coupled with fluorescein labeling (fluorescein isothiocyanate) was used. Detection was performed using fluorescence microscopy (Leica DMI 4000B; Leica Microsystems, Inc., Buffalo Grove, IL, USA). Green fluorescence was observed at 520±20 nm using a standard fluorescence filter.

Observation of autophagosomes in tissue sections by scanning transmission electron microscopy. Prostate tissues were cut into tissue blocks (1 mm^3) and then fixed in 2.5% glutaraldehyde in 0.01 mol/l phosphate buffer at 4˚C for 2 h. Following incubation in 2% osmium tetroxide at 4˚C for additional 2 h, tissue blocks were dehydrated in graded ethanol solutions. Subsequently, ethanol was substituted with propylene oxide for 30 min at room temperature and embedded in epoxy resin. Ultrathin sections (0.1 μm) were double-stained with 1% uranyl acetate and 0.2% lead citrate for 15 min at room temperature and analyzed by transmission electron microscope (JEM-1220; JEOL, LTD., Tokyo, Japan) at 80 kV.

Statistical analysis. All experiments were repeated three times and similar results were obtained. All data of normal distribution were presented as the mean ± standard deviation as indicated and data were analyzed by one-way analysis of variance with Bonferroni post hoc analysis. Data of non-normal distribution were analyzed by Kruskal-Wallis H-tests. Differences between groups were further analyzed by the Nemenyi test. P<0.05 was considered to indicate a statistically significant difference. SPSS v. 11.5 statistical software (SPSS, Inc., Chicago, IL, USA) was used for all statistical analyses.

Results

Measurement of prostate index. The prostate wet weight, volume and prostatic gland exponent (%) in the testosterone group were significantly higher than those in the control group (P<0.05; Table I). The prostate wet weight, volume and prostatic gland exponent (%) in the rapamycin group was significantly reduced compared with those in the testosterone group (P<0.05; Table I).

HE detection of the morphology of rat prostate tissue. Under the microscope, the prostate glands of rats in the testosterone group (Fig. 1A) were compact. Additionally, part of the cavity was expanded, part of the epithelium was pseudostratified, the glandular epithelium was thickened, part of the glandular epithelium was papillary and prominent in the glandular cavity, more stromal cells were present and the small blood vessels were notably expanded compared with the control group. The morphology of the prostate tissue of the rapamycin group was similar to that of the control group with normal arrangement and no obvious thickening of the glandular epithelium; however, the glandular cavity was dilated, deformed and exhibited a small amount of interstitial proliferation (Fig. 1B). The prostate gland in the 3-MA group was enlarged and exhibited an enlarged gland cavity, the gland epithelium was thicker and part of the glandular epithelium was papillary and prominent within the glandular cavity; however, the extent of this was less than that of the testosterone group. Furthermore, interstitial composition of the prostate tissue in the 3-MA group was increased and congestion and edema were observed (Fig. 1C). In the control group, the structure of the prostate gland was clear, the glandular epithelium was a single layer in columnar arrangement and few epithelia were protruding into the lumen of gland epithelium. Interstitial composition of the prostate tissue was relatively small and no congestion or edema was indicated in the control group (Fig. 1D).

Protein expression levels of Bcl-2, LC3-II and caspase-3 in rat prostate tissue according to western blotting. As demonstrated in Fig. 2A and B, western blotting results indicated that the protein expression levels of Bcl-2 in the testosterone group were significantly higher compared with that in the control group (P<0.05). Bcl-2 protein expression levels in the prostate tissue of the 3-MA group were the lowest of all groups and the protein expression levels of caspase-3 in the prostate tissue of the 3-MA group were significantly higher than those in the other three groups (P<0.05). Furthermore, the protein expression levels of LC3-II in the rapamycin group were similar to the control group but significantly higher than that in the 3-MA and testosterone groups (P<0.05).

mRNA expression levels of Bcl-2 and Beclin-1 in prostate tissue according to RT-qPCR. As demonstrated in Fig. 3, RT-qPCR results revealed that the mRNA expression levels of Bcl-2 at 28 days were significantly higher in the testosterone and rapamycin groups than that in the control group (P<0.05). The mRNA expression levels of Bcl-2 after 28 days in the 3-MA

Table I. Rat weight and wet weight, volume and prostate index of prostate tissue of the rats in each group.

Group	n	Rat weight, g	Prostatic gland weight, g	Prostatic gland volume, ml	Prostatic gland exponent, %
Testosterone	10	413±29[a]	1.09±0.21[a]	0.75±0.32[a]	0.26±0.04[a]
Rapamycin	10	329±27	0.48±0.10[b]	0.40±0.08[b]	0.14±0.03[b]
3-MA	10	428±30	0.84±0.18	0.70±0.15	0.19±0.05
Control	10	357±30	0.54±0.09	0.45±0.08	0.15±0.02

Data are presented as mean ± standard deviation. [a]P<0.05 vs. control; [b]P<0.05 vs. testosterone group. 3-MA, 3-methyladenine.

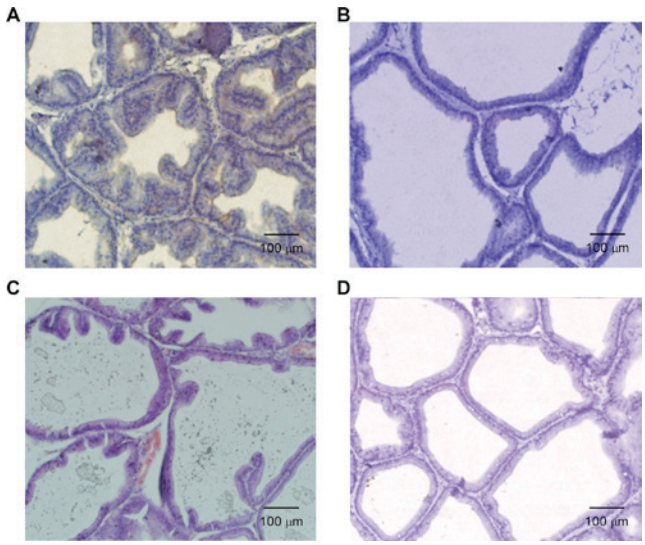

Figure 1. Hematoxylin and eosin staining results of rat prostate tissue after 28 days of treatment in the (A) testosterone, (B) rapamycin, (C) 3-MA and (D) control groups. Magnification, x40. Scale bar, 100 mm. 3-MA, 3-methyladenine.

group were lower than that in the control group, however the result was not significant. As demonstrated in Fig. 4, there was no significant difference in the expression levels of Beclin-1 mRNA between the control and the testosterone groups. The mRNA expression levels of Beclin-1 were significantly lower in the rapamycin and the 3-MA groups than that in the control group (P<0.05).

Level of apoptosis in rat prostate tissues. TUNEL analysis was performed to examine the level of apoptosis in the prostate tissues (Fig. 5). Quantitative analysis of the images revealed that the apoptotic rate of the 3-MA group was significantly increased compared with the control group (P<0.05), whereas the apoptotic rate of prostate tissues in the testosterone and rapamycin groups was significantly decreased compared with the control group (P<0.05; Fig. 6).

Scanning transmission electron microscope observation. At present, it has been suggested that autophagy may be observed using an electron microscope, which is the gold standard to judge the extent of autophagy (13-15). The formation of a lysosome, a vesicle structure with a double membrane, is a vital process of autophagy (14). Some damaged organelles, proteins or glycogen are present inside vesicles (16). When the vesicles are fused with the lysosomal membrane, the inner membrane of the vesicle is hydrolyzed (17). Fusion of the outer membrane of the vesicle and the lysosomal membrane form the autophagy autophagolysosome (17). In the present study, electron microscopy of the rapamycin group revealed that the autophagolysosome contained a single layer of membrane. The ultrathin sections of rat prostate tissue in the rapamycin group were observed under a magnification of x5,000 and revealed that the rat prostate epithelial cells contained autophagolysosomes. In addition, some of the organelles within the autophagosomes in the rapamycin group were not fully digested (Fig. 7). Following injection with 3-MA, the formation of autophagy bodies was not observed in the prostate epithelial cells. Collectively, these results revealed that the level of autophagy was highly activated in rat prostate tissues after rapamycin treatment compared with the control group.

Discussion

BPH is a common disease in men >50 years of age and the incidence of the disease increases with age (1). The pathogenesis of BPH is not yet clear; however, it is closely associated with androgens (18). The growth and development of prostate tissue is associated with the action of androgens and the maintenance of normal prostate tissue morphology must therefore also depend on the role of androgens (19,20). Previous studies have indicated that increased prostate volume is not due to excessive proliferation of prostate tissue, but is instead related to the decrease of apoptosis in prostate tissue (21-23). In adult castrated rats, androgen treatment induces prostatic regrowth, proliferation and increases prostate size (24,25). This method has become a common applied method for the construction of the animal model of BPH (25). In the present study, the wet weight and volume of the prostate of rats after 28 days were measured and the prostate indices of rats in each group were calculated. Results demonstrated that the prostate wet weights, volumes and prostate index in the testosterone group were significantly higher than those in the control group. The results indicated that testosterone successfully induced rat prostate hyperplasia. HE staining results further revealed that, compared with the control group, the prostate glands of the rats in the testosterone group were compact with partially expanded cavities and partially pseudostratified epithelium, the glandular epithelium was thickened, part of the glandular epithelium was papillary and prominent in the glandular cavity with increased

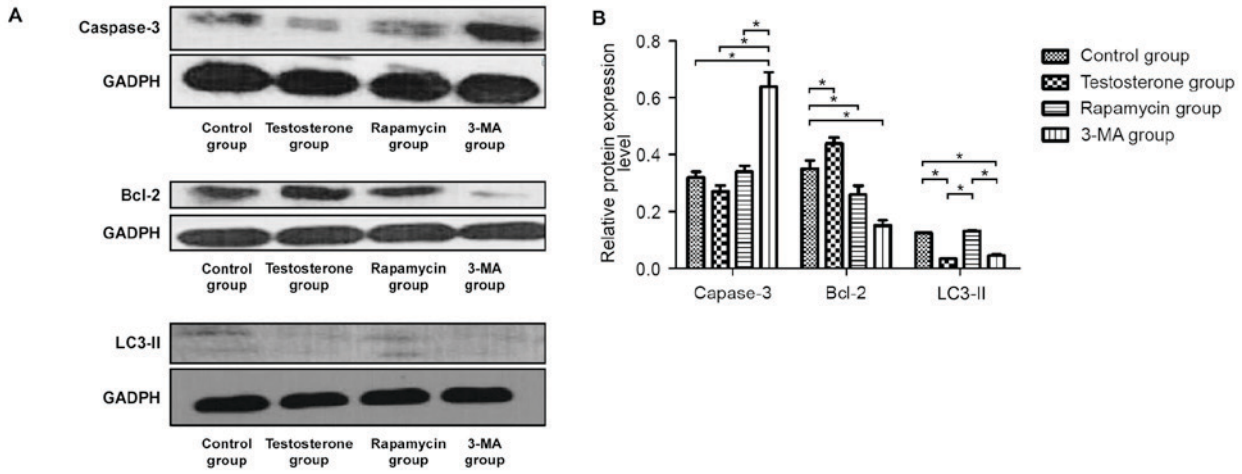

Figure 2. (A) Western blotting and (B) statistical analysis of the protein expression levels of caspase-3, Bcl-2 and LC3-II relative to GAPDH. Data are presented as the mean ± standard deviation. *P<0.05. 3-MA, 3-methyladenine; Blc-2, B-cell lymphoma-2; LC3, microtubule-associated protein 1 light chain 3.

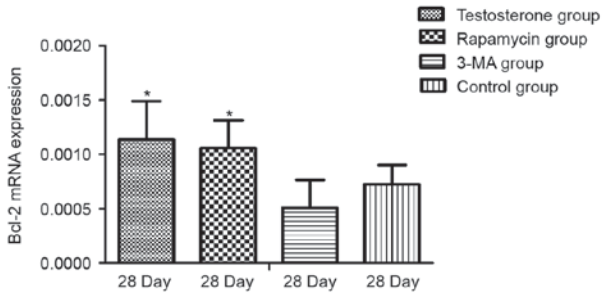

Figure 3. Detection of Bcl-2 mRNA expression levels by reverse transcription-quantitative polymerase chain reaction in rat prostate tissue relative to GAPDH. Data are presented as mean ± standard deviation. *P<0.05 vs. the Control group. 3-MA, 3-methyladenine; Blc-2, B-cell lymphoma 2.

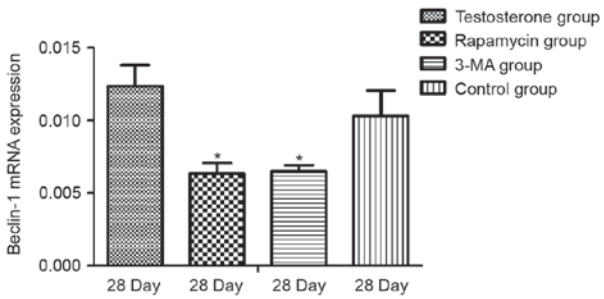

Figure 4. Detection of Beclin-1 mRNA expression levels by reverse transcription-quantitative polymerase chain reaction in rat prostate tissue relative to GAPDH. Data are presented as mean ± standard deviation. *P<0.05 vs. the Control group. 3-MA, 3-methyladenine.

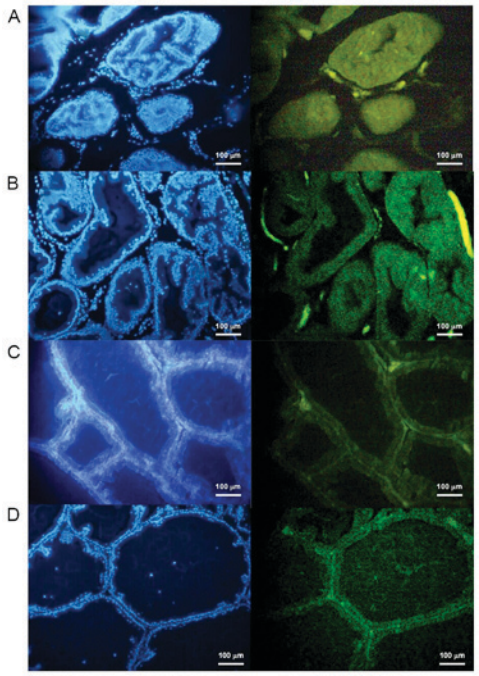

Figure 5. Detection of apoptosis in rat prostate tissue after 28 days of treatment in the (A) testosterone, (B) 3-MA, (C) control and (D) rapamycin groups. 4',6-diamidino-2-phenylindole dye staining was used on the nucleus. When this dye is excited it emits blue light. The fluorescent dye was combined with apoptotic cells and a fluorescence microscope was used to observe the green fluorescence under the excitation of the blue light. Scale bar, 100 mm. Magnification, x40. 3-MA, 3-methyladenine.

stromal cells and expansion of small blood vessels compared with the control group. Prostate tissues in the 3-MA group also exhibited similar changes compared to the testosterone group; however, to a lesser extent. Results demonstrated that the establishment of the present model was successful. In the rapamycin group, the structure of the prostate was normal, the glands were closely arranged, the size of the cavity was normal and the glandular epithelium was not raised. Compared with the control group, the interstitial composition in the rapamycin group was slightly increased; however, no vascular congestion was detected and the epithelial cells were in a single arrangement with no pseudostratified epithelial formation. Compared with the testosterone and control groups, no notable prostate tissue proliferation was observed in the prostate tissue of the rapamycin group. Therefore, we propose that rapamycin may inhibit the proliferation of prostate tissue in rats induced by testosterone.

Currently, it is not known whether androgen-induced prostate hyperplasia in rats is promoted by the excessive proliferation of prostate tissue or by the reduction of prostate

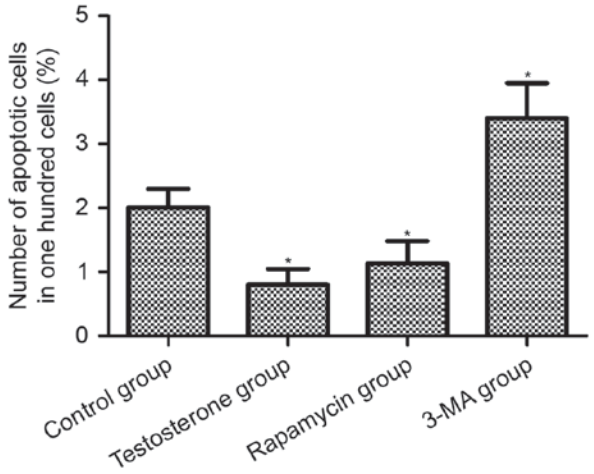

Figure 6. Rate of apoptosis in rat prostate tissue after 28 days of treatment. The longitudinal axis represents the number of apoptotic cells per 100 cells in a microscopic field (magnification, x40). Data are presented as mean ± standard deviation. *P<0.05 vs. the Control group. 3-MA, 3-methyladenine.

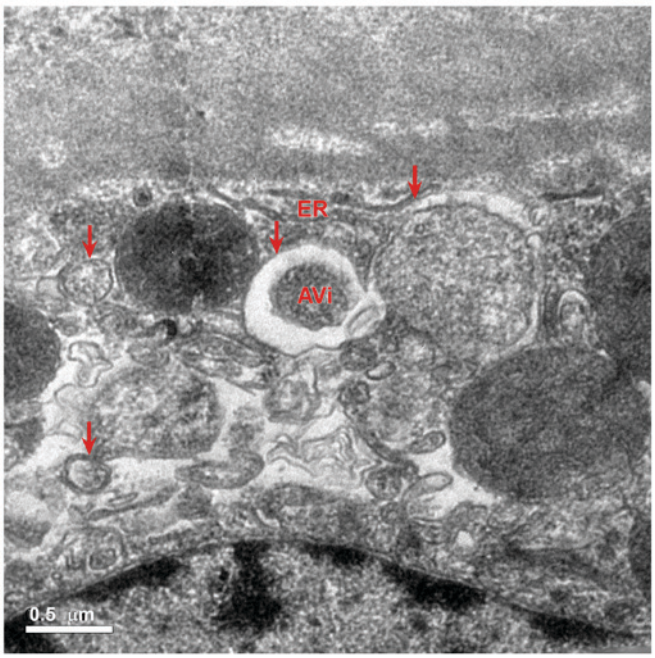

Figure 7. Electron microscopic observation of prostate tissue of rapamycin group after 28 days of treatment (magnification, x5,000). Ultrathin sections were double-stained with 1% uranyl acetate and 0.2% lead citrate and analyzed by transmission electron microscopy. Red arrows indicate autophagy. Under the electron microscope, vesicles with a single layer membrane structure in the cells were observed. Incomplete digested organelles and other contents were also observed in the autophagosome. Scale bar, 0.5 μm. AVi, autophagosomes or initial autophagic vacuoles; ER, endoplasmic reticulum.

tissue apoptosis; therefore, this was a primary investigation in the present study. Western blotting results demonstrated that, compared with the control group, androgen was able to decrease the expression of caspase-3, increase the expression of Bcl-2 protein and reduce the expression of LC3-II protein in prostate tissue. TUNEL assay results demonstrated that, compared with the control group, the rate of apoptosis in the prostate tissues of rats in the testosterone and the rapamycin groups were significantly decreased. These results indicated that androgen was able to decrease the rate of apoptosis and autophagy in the prostate tissue of castrated rats.

Androgen regulates the growth, proliferation and death of prostate cancer cells, which may be associated with androgen receptor (AR) function and the phosphoinositide 3-kinase/protein kinase B/mechanistic target of rapamycin (PI3K/Akt/mTOR) signaling pathway (26). Both AR and PI3K/Akt/mTOR signaling influence the proliferation and death of prostate cancer cells and feedback to each other (27). Kinkade *et al* (28) have identified that targeting Akt/mTOR and ERK/MAPK signaling pathways inhibits androgen-independent prostate tumors in the mouse model. This research proposed that inhibition of the Akt/mTOR and ERK/MAPK signaling pathways produces a wide range of therapeutic effects on prostate cancer, particularly concerning androgen-resistant prostate cancer, in the advanced stages (28). In order to verify the assumption that androgen is related to the PI3K-1/Akt/mTOR pathway, testosterone propionate was excessively injected into rats of the testosterone group, and rapamycin was used to inhibit the PI3K/Akt pathway in the rapamycin group. The present results revealed that rapamycin was able to inhibit the effect of androgen. Compared with the control group, the weight of rats was significantly increased 28 days after injections with testosterone propionate, which may be related to the role of androgen in promoting the growth of rat skeletal muscle (29,30). Rapamycin was used to block the PI3K-1/Akt/mTOR pathway and the same dose of testosterone was injected in rats of the rapamycin group. Compared with the control group, there was no significant change in the weight of the rats in the rapamycin group. Western blotting results demonstrated that the expression levels of caspase-3 and Bcl-2 protein in the prostate cells of the rapamycin group were higher and lower, respectively, than those in the testosterone group. The role of testosterone may be related to the PI3K-1/Akt/mTOR pathway (31).

The present study demonstrated that rapamycin blocked the PI3K/Akt/mTOR pathway *in vivo,* which may affect the role of testosterone in promoting skeletal muscle growth. These results were similar to findings from a corresponding *in vitro* study (28) and further supported that the signaling pathway for androgen is related to the PI3K-1/Akt/mTOR pathway. Androgen may improve the level of protein synthesis and promote cell growth and proliferation in prostate tissue by activating the PI3K-1/Akt/mTOR pathway. This may therefore result in a decrease in the rate of apoptosis.

The relationship between autophagy and apoptosis is complex. Increasing the level of autophagy in tumor tissue may decrease the rate of apoptosis in tumor cells (32). The reason is that the survival ability of tumor cells in an unfavorable environment, such as that created by radiotherapy and chemotherapy, is enhanced due to the enhanced autophagy (33). The rate of prostate cancer cell apoptosis appears to bottleneck in response to endocrine therapy characterized by a decrease that is not sustained (34). Therefore, various researchers have proposed autophagy inhibition as a possible clinical strategy to counteract therapeutic resistance in prostate cancer (34).

In the process of androgen-induced prostatic hyperplasia in rats, the extent to which the level of autophagy affects the role of androgen has not been reported. Rapamycin is

a common inducer of autophagy and also has the ability to block the PI3K-1/Akt/mTOR pathway (35). Rapamycin is able to inhibit mTOR protein and therefore promote autophagy. At present, the formation of autophagy bodies is the gold standard to judge the occurrence of autophagy (36,37). Rat prostate tissue was observed using an electron microscope after injection of testosterone and rapamycin in rats for 28 days. In the rapamycin group, autophagolysosomes were observed. Some of the organelles had not been fully digested and were located inside the autophagolysosome. In the control, testosterone and 3-MA groups, autophagolysosomes were not observed. Western blotting results demonstrated that the expression level of LC3-II protein in the rat prostate tissue of the rapamycin group was similar to that in the control group, which suggested that rapamycin induces autophagy activation. In contrast, autophagy was inhibited in rat prostate tissue in the 3-MA group by 3-MA. Results indicated that rapamycin inhibited the role of androgen in promoting the proliferation of prostate tissue in rats by stimulating autophagy. Compared with the control group, there was no obvious prostate hyperplasia in the rapamycin group. However, autophagy inhibition by 3-MA promoted hyperplasia in the 3-MA-treated rat prostate tissues. In addition, the level of apoptosis in the rat prostate tissues was increased compared with that in the control group.

In conclusion, the results of the present study suggested that androgen-induced prostate hyperplasia in rats is not only related to testosterone inhibition of prostate cell apoptosis, it is also possible that testosterone promotes excessive proliferation of prostate tissue in rats. Furthermore, rapamycin may promote the level of autophagy and inhibit the proliferation of prostate tissue in rats, which is not induced by the promotion of apoptosis.

Acknowledgements

The present study was supported by the Medical Elite Cultivation Program of Fujian (Fujian, China; grant no. 2014-ZQN-ZD-33).

References

1. Dhingra N and Bhagwat D: Benign prostatic hyperplasia: An overview of existing treatment. Indian J Pharmacol 43: 6-12, 2011.
2. Lepor H: Pathophysiology, epidemiology and natural history of benign prostatic hyperplasia. Rev Urol 6: S3-S10, 2004.
3. Suzuki S, Platz EA, Kawachi I, Willett WC and Giovannucci E: Intake of energy and macronutrients and the risk of benign prostatic hyperplasia. Am J Clin Nutr 75: 689-697, 2002.
4. Golda R, Wolski Z, Wyszomirska-Golda M, Madaliński K and Michałkiewicz J: The presence and structure of circulating immune complexes in patients with prostate tumors. Med Sci Monit 10: CR123-CR127, 2004.
5. Vignozzi L, Rastrelli G, Corona G, Gacci M, Forti G and Maggi M: Benign prostatic hyperplasia: A new metabolic disease? J Endocrinol Invest 27: 1380-1384, 2014.
6. Turcu A, Smith JM, Auchus R and Rainey WE: Adrenal androgens and androgen precursors: Definition, synthesis, regulation and physiologic actions. Compr Physiol 4: 1369-1381, 2014.
7. Bhutia SK, Das SK, Azab B, Dash R, Su ZZ, Lee SG, Dent P, Curiel DT, Sarkar D and Fisher PB: Autophagy switches to apoptosis in prostate cancer cells infected with melanoma differentiation associated gene-7/interleukin-24 (mda-7/il-24). Autophagy 7: 1076-1077, 2011.
8. Lian J, Wu X, He F, Karnak D, Tang W, Meng Y, Xiang D, Ji M, Lawrence TS and Xu L: A natural bh3 mimetic induces autophagy in apoptosis-resistant prostate cancervia modulating bcl-2-beclin1 interaction at endoplasmic reticulum. Cell Death Differ 18: 60-71, 2011.
9. Wang Y, Shao JC and Zhang SW: Histomorphological studies on hyperplastic prostate of castrated rat caused by androgen. Zhonghua Nan Ke Xue 8: 190-193, 2001 (In Chinese).
10. Scolnik MD, Servadio C and Abramovici A: Comparative study of experimentally induced benign and atypical hyperplasia in the ventral prostate of different sat strains. J Androl 15: 287-297, 1994.
11. Wei XY, Zhang JK, Li J and Chen SB: Effect of bilateral testicular resection on thymocyte and its microenvironment in aged mice. Asian J Androl 3: 271-275, 2001.
12. Livak KJ and Schmittgen TD: Analysis of relative gene expression data using real-time quantitative PCR and the 2(-Delta Delta C(T)) method. Methods 25: 402-408, 2001.
13. Bizargity P and Schröppel B: Autophagy: Basic principles and relevance to transplant immunity. Am J Transplant 14: 1731-1739, 2014.
14. Todde V, Veenhuis M and van der Klei IJ: Autophagy: Principles and significance in health and disease. Biochim Biophys Acta 1792: 3-13, 2009.
15. Mizushima N: Autophagy: Process and function. Genes Dev 21: 2861-2873, 2007.
16. Wrighton KH: Eating up damaged lysosomes. Nat Rev Mol Cell Biol 14: 465, 2013.
17. Münz C: The Autophagic machinery in viral exocytosis. Front Microbiol 8: 269, 2017.
18. Moore A, Butcher MJ and Köhler TS: Testosterone replacement therapy on the natural history of prostate disease. Curr Urol Rep 16: 51, 2015.
19. Singh M, Jha R, Melamed J, Shapiro E, Hayward SW and Lee P: Stromal androgen receptor in prostate development and cancer. Am J Pathol 184: 2598-2607, 2014.
20. Zhou Y, Bolton EC and Jones JO: Androgens and androgen receptor signaling in prostate tumorigenesis. J Mol Endocrinol 54: R15-R29, 2015.
21. Quiles MT, Arbós MA, Fraga A, de Torres IM, Reventós J and Morote J: Antiproliferative and apoptotic effects of the herbal agent pygeumafricanumon cultured prostate stromal cells from patients with benign prostatic hyperplasia (BPH). Prostate 70: 1044-1053, 2010.
22. Boya P and Kroemer G: Beclin 1: A BH3-only protein that fails to induce apoptosis. Oncogene 28: 2125-2127, 2009.
23. Ciechomska IA, Goemans GC, Skepper JN and Tolkovsky AM: Bcl-2 complexed with Beclin-1 maintains full anti-apoptotic function. Oncogene 28: 2128-2141, 2009.
24. Nicholson TM and Ricke WA: Androgens and estrogens in benign prostatic hyperplasia: Past, present and future. Differentiation 82: 184-199, 2011.
25. Oudot A, Oger S, Behr-Roussel D, Caisey S, Bernabé J, Alexandre L and Giuliano F: A new experimental rat model of erectile dysfunction and lower urinary tract symptoms associated with benign prostatic hyperplasia: The testosterone-supplemented spontaneously hypertensive rat. BJU Int 110: 1352-1358, 2012.
26. Liao RS, Ma S, Miao L, Li R, Yin Y and Raj GV: Androgen receptor-mediated non-genomic regulation of prostate cancer cell proliferation. Transl Androl Urol 2: 187-196, 2013.
27. Floc'h N and Abate-Shen C: The promise of dual targeting Akt/mTOR signaling in lethal prostate cancer. Oncotarget 3: 1483-1484, 2012.
28. Kinkade CW, Castillo-Martin M, Puzio-Kuter A, Yan J, Foster TH, Gao H, Sun Y, Ouyang X, Gerald WL, Cordon-Cardo C and Abate-Shen C: Targeting AKT/mTOR and ERK MAPK signaling inhibits hormone-refractory prostate cancer in a preclinical mouse model. J Clin Investig 118: 3051-3064, 2008.
29. Michel G and Baulieu EE: Androgen receptor in rat skeletal muscle: Characterization and physiological variations. Endocrinology 107: 2088-2098, 1980.
30. Fu R, Liu J, Fan J, Li R, Li D, Yin J and Cui S: Novel evidence that testosterone promotes cell proliferation and differentiation via G protein-coupled receptors in the rat L6 skeletal muscle myoblast cell line. J Cell Physiol 227: 98-107, 2012.
31. Basualto-Alarcón C, Jorquera G, Altamirano F, Jaimovich E and Estrada M: Testosterone signals through mTOR and androgen receptor to induce muscle hypertrophy. Med Sci Sports Exerc 45: 1712-1720, 2013.

32. Lorenzo PI and Saatcioglu F: Inhibition of apoptosis in prostate cancer cells by androgens is mediated through downregulation of c-Jun N-terminal kinase activation. Neoplasia 10: 418-428, 2008.
33. Wang Z, Du T, Dong X, Li Z, Wu G and Zhang R: Autophagy inhibition facilitates erlotinib cytotoxicity in lung cancer cells through modulation of endoplasmic reticulum stress. Int J Oncol 48: 2558-2566, 2016.
34. Ziparo E, Petrungaro S, Marini ES, Starace D, Conti S, Facchiano A, Filippini A and Giampietri C: Autophagy in prostate cancer and androgen suppression therapy. Internat J Mol Sci 14: 12090-12106, 2013.
35. Heras-Sandoval D, Pérez-Rojas JM, Hernández-Damián J and Pedraza-Chaverri J: The role of PI3K/AKT/mTOR pathway in the modulation of autophagy and the clearance of protein aggregates in neurodegeneration. Cell Signal 26: 2694-2701, 2014.
36. Klionsky DJ, Abdelmohsen K, Abe A, Abedin MJ, Abeliovich H, Acevedo Arozena A, Adachi H, Adams CM, Adams PD and Adeli K, *et al*: Guidelines for the use and interpretation of assays for monitoring autophagy (3rd edition). Autophagy 12: 1-222, 2016.
37. Huang CC, Lee CC, Lin HH, Chen MC, Lin CC and Chang JY: Autophagy-regulated ROS from xanthine oxidase acts as an early effector for triggering late mitochondria-dependent apoptosis in cathepsin S-targeted tumor cells. PLoS One 10: e0128045, 2015.